



Design and Analysis of Novel Folded Optical Multi-Pass Cell

Gang Cheng¹, Ya-Nan Cao^{1,2*}, Xing Tian¹, Jia-Jin Chen³ and Jing-Jing Wang⁴

¹State Key Laboratory of Mining Response and Disaster Prevention and Control in Deep Coal Mines, Anhui University of Science and Technology, Huainan, China, ²Institute of Environment-Friendly Materials and Occupational Health of Anhui University of Science and Technology, Wuhu, China, ³Anhui Institute of Optics and Fine Mechanics, Chinese Academy of Sciences, Hefei, China, ⁴Institute of Atmospheric Science, Fudan University, Shanghai, China

A novel folded multi-pass cell consisting of three non-coaxial mirrors (spherical mirror or plane mirror) is proposed for laser spectroscopy. Three mirrors of the folded multi-pass cell can arrange in V-shape to form a stable non-coaxial multi-pass cell. Furthermore, in order to research the stability of the multi-pass cell under off-axis mirror's astigmatism circumstance, an equivalent coaxial multi-pass cell and modified ABCD matrix model for the spot pattern of the folded multi-pass cell is proposed, by which a series of the detailed numerical calculations were implemented to analyze the optical path length of the multi-pass cell. Many spot patterns obtained with a high fill factor improve the utilization efficiency of the surface of the mirror and produce a longer total optical path length. The several typical types of folded multi-pass cells consisting of the different mirrors and base lengths were selected to demonstrate the cell's self-consistent condition and power for a longer-optical path length. Three effective optical path lengths of 49.6, 97.6 and 173.6 m were obtained, respectively.

OPEN ACCESS

Edited by:

Yufei Ma,
Harbin Institute of Technology, China

Reviewed by:

Yahui Liu,
Harbin Institute of Technology, China

Wu Zhenwei,
Hefei Institutes of Physical
Science(CAS), China

*Correspondence:

Ya-Nan Cao
cynpf@mail.ustc.edu.cn

Specialty section:

This article was submitted to
Optics and Photonics,
a section of the journal
Frontiers in Physics

Received: 30 March 2022

Accepted: 15 April 2022

Published: 17 June 2022

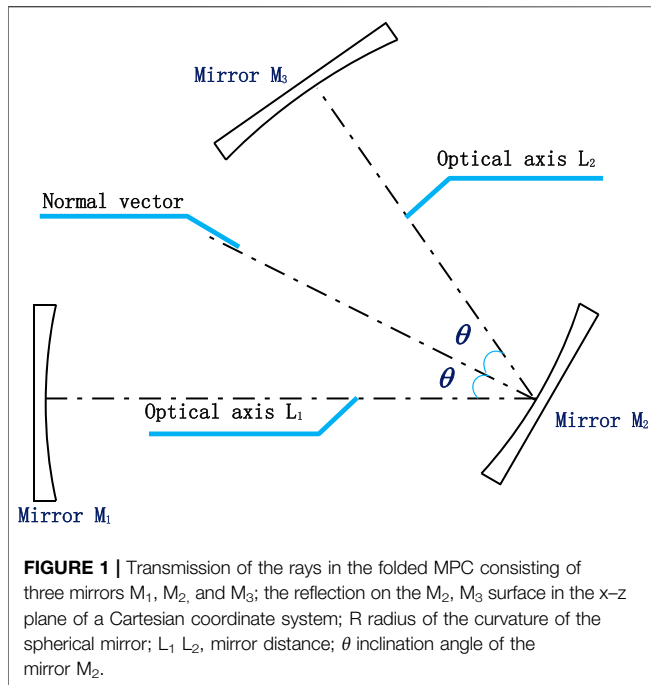
Citation:

Cheng G, Cao Y-N, Tian X, Chen J-J
and Wang J-J (2022) Design and
Analysis of Novel Folded Optical Multi-
Pass Cell.
Front. Phys. 10:907715.
doi: 10.3389/fphy.2022.907715

Keywords: folded multi-pass cell, non-coaxial mirror, modified ABCD matrix, dense spot pattern, long optical path length

INTRODUCTION

The multi-pass cell (MPC) is regarded as an important part of laser absorption spectroscopy for an effective long optical path length (OPL). In addition, due to its real-time online, high sensitivity, high selectivity non-contracted and non-intrusive advantages, the laser absorption spectroscopy is widely used in the fields of atmosphere, environmental pollution, and industrial process, industrial emissions for trace gas chemical composition analysis, and measurement (CH₄, CO₂, CO, HCHO, N₂O, NH₃, etc.) [1–10]. Early White cells, Herriot cells, and Chernin cells [11–13] are still used in a laser-based spectroscopic trace gas sensor due to the advantages of the MPC. The White cells, Herriot cells, and Chernin cells have some drawbacks, such as a relatively large volume, low effective utilization areas of mirrors and complex structure, which limits their application in miniaturization instruments. Considering the advantages of the MPC in laser spectroscopy, the design of miniaturized and weight light MPC will be one of the mainstream development trends in the future. For more compact size and longer OPL, recently, many various MPCs have been reported and developed, in which at least one spherical mirror was replaced with an aspherical mirror. In 2013, BélaTuzson et al. [14, 15] developed a toroidal MPC, which consisted of a single piece of reflective toroidal surface forming a near-concentric cavity in a circular configuration with a volume of merely 40 ml, for this new type of MPC, two effective OPLs of 2.2 and 4.1 m were chosen to demonstrate the cell's suitability. In 2015, Liu et al. [16] designed a novel compact dense-pattern multi-pass cell (DP-MPC) with a 280 ml sampling volume, whose minimum detectable



concentration of 100 ppb was obtained. In 2016, Dong et al. [17–19] developed the ultra-compact multi-pass gas cell, which offered a 54.6 m OPL in physical size of $17 \times 6.5 \times 5.5 \text{ cm}^3$ with a 220 ml sampling volume. In 2017, Ozharar et al. [20] designed an aspherical MPC, in which the focal length of aspherical mirrors varied inversely to the ray height from the optical axis, for aspherical MPC a very rich set of exotic spot patterns can be formed on the end mirrors by numerical simulations. In 2019, Kong et al. [21] reported a new design method for the multi-pass cell with a similar traditional configuration. For instance, the OPL is 20.4 m after the beam passes 183 times in the cell, and the sample volume is approximately 332.1 ml. In 2020, Cui et al. [22] reported three-dimensional printed miniature fiber-coupled multipass cells with an optical absorption path length of 4.2 m and dimensions of $4 \times 4 \times 6 \text{ cm}^3$. A limitation of laser absorption spectroscopy originates from the requirement of the long OPL, especially when detecting the low concentrations of the trace gas on the order of ppm. In this article, a novel folded multi-pass cell consisting of three non-coaxial mirrors is presented. Three mirrors of the folded multi-pass cell can arrange in V-shape to form a stable non-coaxial multi-pass cell. Furthermore, in order to research the self-consistent condition of the multi-pass cell and the number of reflections, an equivalent coaxial multi-pass cell and modified ABCD matrix model for the spot pattern of the folded multi-pass cell is proposed, by which a series of the detailed numerical calculations were implemented to analyze the optical path length of the multi-pass cell. Due to the off-axis mirror's astigmatism, many dense spot patterns obtained with a high fill factor produce a longer total optical path length. The folded multi-pass cell with dense patterns shows superior characteristics, such as small volume, simple structure, long effective OPL, high detection sensitivity, and affordable cost,

which make them very suitable for various field applications, particularly for trace gas sensing. The proposed MPCs can overcome the disadvantage of the number of reflection times possible for the Herriott cell and can achieve up to hundreds of reflections with a small overlap. Despite the optical interference fringes due to the small overlap tend to cause difficulties in multi-pass absorption spectroscopy and limit its sensitivity. The optical interference fringes can be effectively suppressed by wavelength-modulation spectroscopy (WMS) and frequency-modulation spectroscopy (FMS) [23].

OPTICAL SETUP OF THE FOLDED OPTICAL MULTI-PASS CELL

The optical setup for a novel folded optical multi-pass cell is shown in **Figure 1**. First, the incident ray transmits between two spherical mirrors (M_1 and M_2) and then reflects from the M_2 surface to the spherical mirror (M_3) surface; after that reflects from M_3 to M_2 ; at the last, the ray is transmitted to M_1 surface to complete a pass count in the structure of the folded MPC.

Compared with the coaxial MPC, the non-coaxial MPC is much more complicated. In order to simplify the analysis of complicated non-coaxial MPC, according to the theory of laser cavity, an equivalent coaxial multi-element MPC is proposed as displayed in **Figure 2**.

An equivalent cavity consists of two spherical mirrors and a lens that possesses different focal lengths in the meridian plane and sagittal plane due to the astigmatism of the off-axis spherical mirror M_2 . In the meridian plane and sagittal plane, the focal length is defined as $f_m = 0.5 R \cos(2\theta)$, $f_s = 0.5 R \sec(2\theta)$, respectively. If the astigmatism of the off-axis spherical mirror is not considered, a set of beautiful spot patterns on the mirrors cannot be calculated by a numerical calculation model based on the ABCD matrix.

CALCULATION MODEL OF THE SPOT PATTERN OF THE FOLDED OPTICAL MULTI-PASS CELL

In this paper, in consideration of the astigmatism of the off axis spherical mirror (M_2), the modified 4×4 ABCD matrix describing one complete pass count is proposed, which consists of the standard transmission matrix and the standard reflection matrix of the ray:

$$M = \begin{bmatrix} A & B \\ C & D \end{bmatrix} = \begin{bmatrix} 1 & 0 & 0 & 0 \\ -\frac{2}{R} & 0 & 1 & 0 \\ 0 & 1 & 0 & 0 \\ 0 & -\frac{2}{R} & 0 & 1 \end{bmatrix} * \begin{bmatrix} a & b \\ c & d \end{bmatrix} * \begin{bmatrix} 1 & 0 & 0 & 0 \\ -\frac{2}{R} & 0 & 1 & 0 \\ 0 & 1 & 0 & 0 \\ 0 & -\frac{2}{R} & 0 & 1 \end{bmatrix} \quad (1)$$

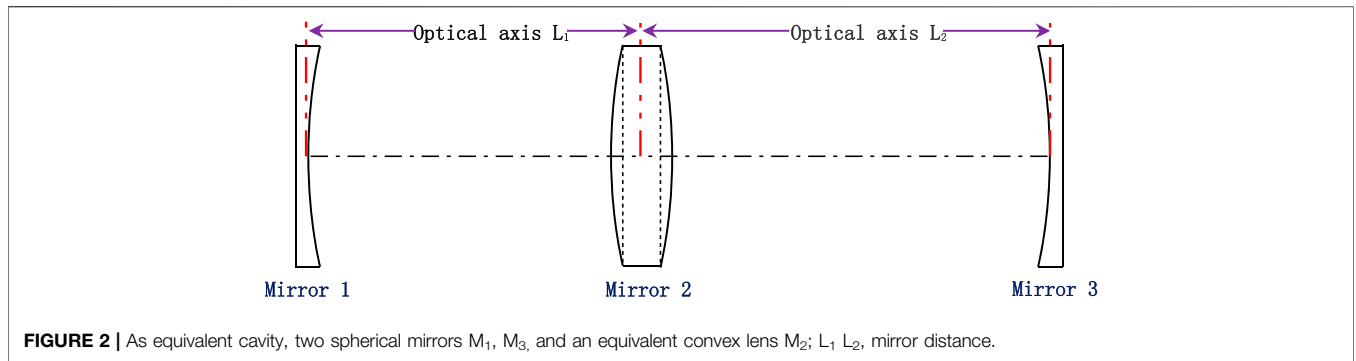


FIGURE 2 | As equivalent cavity, two spherical mirrors M_1 , M_3 , and an equivalent convex lens M_2 ; L_1 L_2 , mirror distance.

$$m = \begin{bmatrix} a & b \\ c & d \end{bmatrix}$$

$$= \begin{bmatrix} 1 & 0 & L_1 & 0 \\ 0 & 0 & 1 & 0 \\ 0 & 1 & 0 & L_1 \\ 0 & 0 & 0 & 1 \end{bmatrix} * \begin{bmatrix} 1 & 0 & 0 & 0 \\ \frac{-1}{f_m} & 0 & 1 & 0 \\ 0 & 1 & 0 & 0 \\ 0 & \frac{-1}{f_s} & 0 & 1 \end{bmatrix} * \begin{bmatrix} 1 & 0 & L_2 & 0 \\ 0 & 0 & 1 & 0 \\ 0 & 1 & 0 & L_2 \\ 0 & 0 & 0 & 1 \end{bmatrix} \quad (2)$$

where $m = [a \ b; c \ d]$ is expressed as a one-way ABCD matrix in the cell.

If an incident ray enters the MPC from M_1 with the initial parameters (x_0, x'_0) , (y_0, y'_0) on the M_1 surface. x_0, y_0, x'_0, y'_0 serve as incident location and inclination angle, respectively. After n pass counts, a ray is described by the coordinates (x_{n-1}, x'_{n-1}) , (y_{n-1}, y'_{n-1}) of the point where it is located on the spherical mirror's surface.

$$(x_{n-1}, y_{n-1}, x'_{n-1}, y'_{n-1}) = \begin{bmatrix} A & B \\ C & D \end{bmatrix}^n (x_0, y_0, x'_0, y'_0) \quad (3)$$

CONFINEMENT STABILITY OF THE FOLDED OPTICAL MPC

The theoretical study of the self-consistent condition of the MPC is the first step before designing any optical MPC (choice of the curvature radius, base length of the cell). Based on laser cavity theory, the optical cavity's eigenvalue method used to judge the stability of the cell is more concise. Taking one mirror as the reference plane, the corresponding eigenvalue λ of the ABCD matrix of the equivalent MPC in the meridian plane or the sagittal plane is determined by Eqs 4–6. The criterion for a stable cell or cavity can be strictly exhibited as follow:

$$\left| \begin{bmatrix} A - \lambda E & B \\ C & D - \lambda E \end{bmatrix} \right| = 0 \quad (4)$$

$$\lambda^2 - (A + D)\lambda + 1 = 0 \quad (5)$$

$$\lambda_{1,2} = \frac{A + D}{2} \pm \sqrt{\left(\frac{A + D}{2}\right)^2 - 1} \quad (6)$$

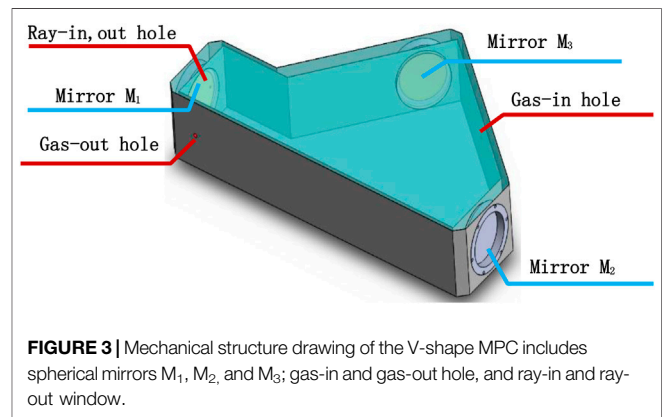


FIGURE 3 | Mechanical structure drawing of the V-shape MPC includes spherical mirrors M_1 , M_2 , and M_3 ; gas-in and gas-out hole, and ray-in and ray-out window.

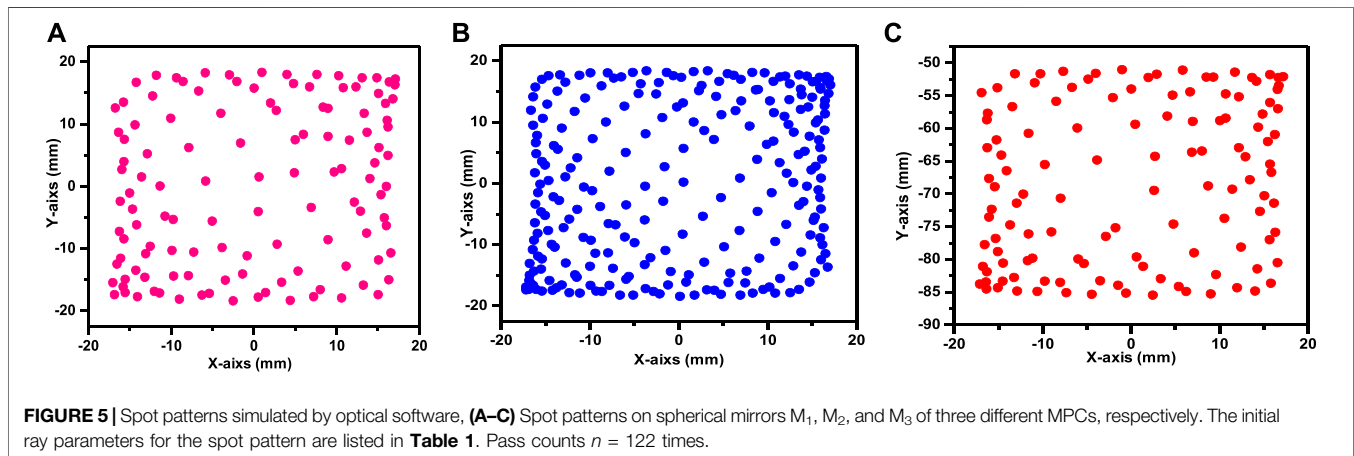
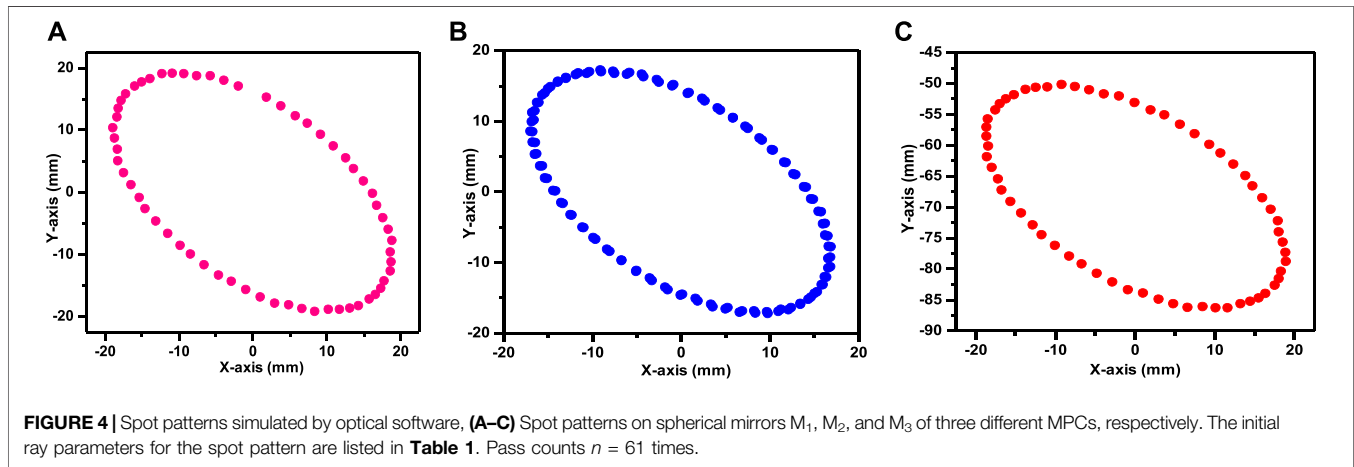
When the $|A + D| > 2$, it is found that the lambda λ consists of a pair of real numbers, which means that in a cycle the ray (x_0, x'_0) or (y_0, y'_0) is at magnification (decrease) of λ times. So, under the self-consistent condition, the ray will diverge (converge) into a point-source of ray in the cavity, which is called an unstable cavity. When the $|A + D| < 2$, it is concluded that the lambda λ consists of a pair of conjugate complex numbers, whose real part and imaginary part stand for the curvature of the wavefront and the radius of the ray spot, respectively, according to the diagonalization of the complex wavefront. therefore, the optical cavity is stable.

OPTICAL ARRANGEMENT OF THE FOLDED OPTICAL MULTI-PASS CELL

The optical arrangement of the folded MPC involving three identical spherical mirrors is shown in Figure 3. As a requirement to get a long OPL, three high reflectivity dielectric-coating spherical mirrors (reflectivity of 99.993% at the wavelength of 1.573 μm) are employed to form a folded MPC. The three identical spherical mirrors have a diameter of (50.8 mm) and a radius of (1,000 mm), which are non-coaxial arrangements, and the arm's base lengths L_1 and L_2 are 150 mm, 200 mm, respectively. The spherical mirror M_1 and M_3 are 90° angles to the optical axis respectively, which is equivalent to θ with a value of 10° as shown in Figure 1. Around the MPC, there

TABLE 1 | Incident location (x_0 , y_0 , z_0), Incident vector (x' , y' , z'), Curvature radius (R) of three mirrors, M_2 , M_3 , Mirrors separated distance (L_1), (L_2), Volume (V) and Ratio (RLV) used to obtain the spot patterns depicted in **Figures 4, 9**.

Pattern	(x_0, y_0, z_0) (mm)	(x', y', z')	L_1 (mm)	L_2 (mm)	R (mm)			OPL (m)	V (cm ³)	RLV (cm ⁻²)
					M_1	M_2	M_3			
Figure 4	(0, 16, -199.5)	(-0.08, 0.008, 2.1)	2*102	2*102	103	∞	103	49.6	950	5
Figure 5	(16, 16, 209)	(0.007, 0.007, 2.1)	2*102	2*102	103	103	103	97.6	950	10
Figure 6	(15, 16, -155)	(0.008, 0.007, 1.5)	1.5*102	2*102	103	103	103	173.6	780	22

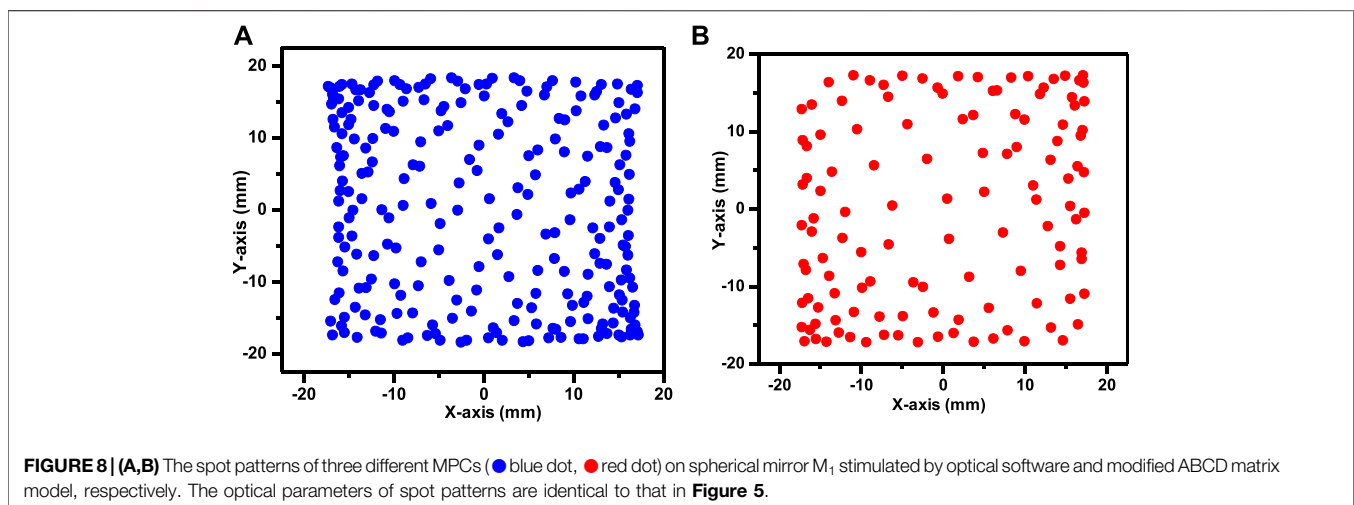
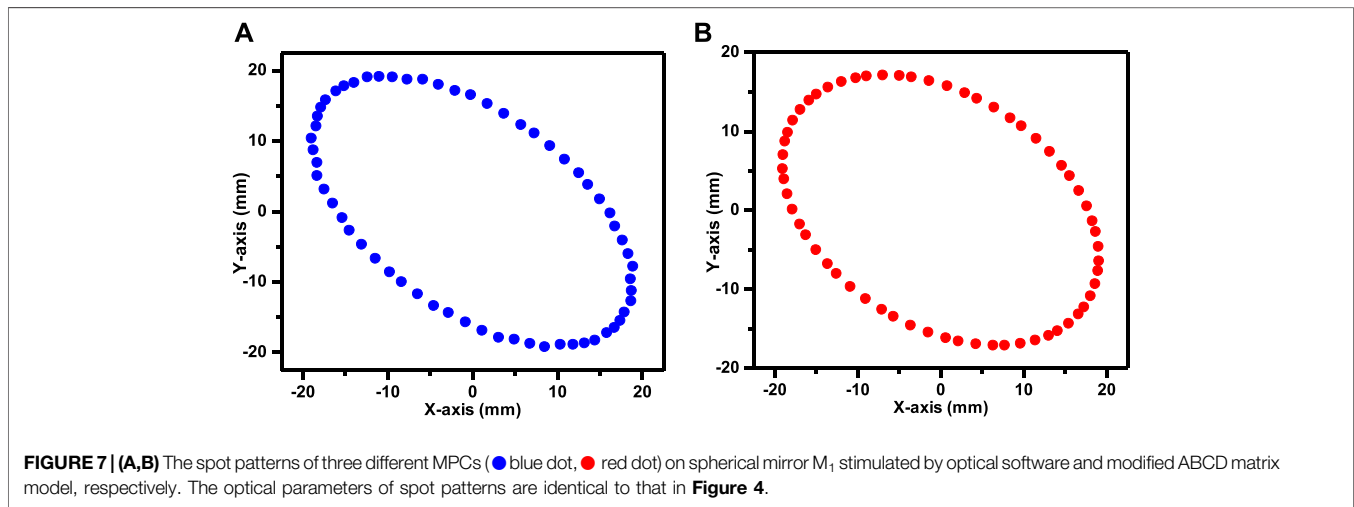
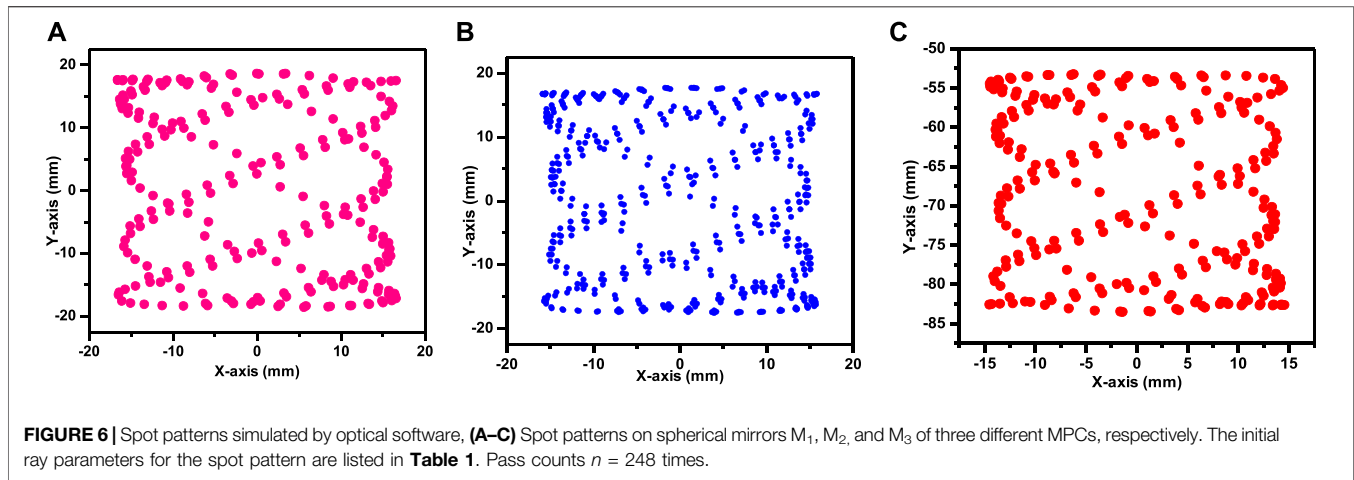


are gas-in and gas-out holes for gas change. The spherical mirror M_1 possess ray-in and ray-out windows as displayed in the mechanical structure drawing **Figure 3**.

RESULTS AND DISCUSSION

Three typical folded MPC are selected to show, whose eigenvalue λ is the conjugate complex numbers with value of $(-0.28 \pm 0.9600i, -0.28 \pm 0.9600i)$, $(-0.8487 \pm 0.5289i, -0.8377 \pm 0.5461i)$, $(-0.7524 \pm 0.6588i, -0.7393 \pm 0.6734i)$, respectively,

which means that those folded MPCs selected to show is stable. On the base of the stable cavity, by adjusting incident ray's parameters such as initial incident angle, initial entry location on M_1 , mirrors separated distance (L_1) or distance (L_2) between mirrors, some satisfying number of the reflections on x-y plane of the mirrors can be obtained. Therefore, it is demonstrated that an original folded MPC is powerful to create a long OPL. In the calculation model, with a fixed inclination angle θ (10°) of the spherical mirror M_2 , the longest OPL is the spot pattern of **Figure 6** with a value of 173.6 m. In fact, a ratio of the total OPL to the volume can better reflect the space utilization of the



ray in the MPC. According to the ratio of OPL to V (RLV) in **Table 1**, the most efficient space utilization is the spot pattern with a value of 22 in **Figure 6**. Those extraordinary spot patterns

result mainly from the astigmatism of the off-axis spherical mirror M_2 , which plays an important role in the spot pattern evolution caused by the off-axis spherical mirror's astigmatism.

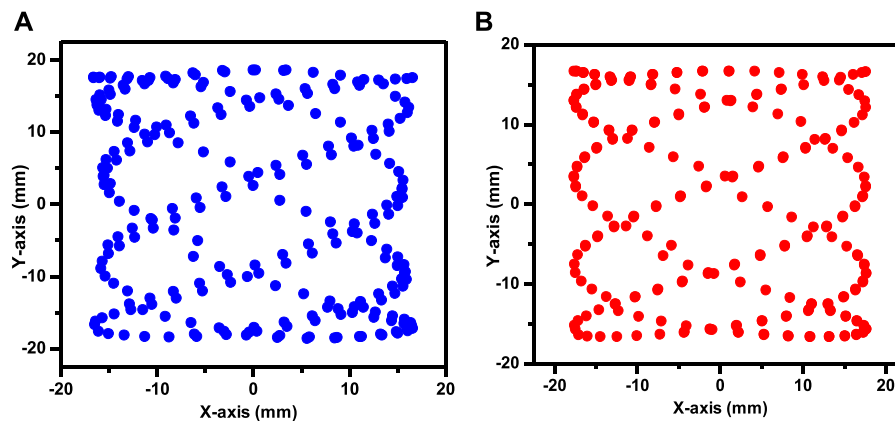


FIGURE 9 | (A,B) The spot patterns of three different MPCs (● blue dot, ● red dot) on spherical mirror M_1 stimulated by optical software and modified ABCD matrix model, respectively. The optical parameters of spot patterns are identical to that in **Figure 6**.

When the important ray's parameter such as the incident location (x_0, y_0, z_0), incident vector (x', y', z'), mirrors spacing (L_1, L_2), and curvature radius (R) is depicted in **Table 1** of the spherical mirrors, each spot pattern in **Figures 4–6** can evolve more spot patterns to increase the spot density or down. In **Figures 4, 6** the pass counts are 61 times, 122 times, and 248 times, respectively. It is found that the number of the reflection of the ray on the M_2 is twice as much as that on the M_1, M_3 mirror surface due to the folded MPC consisting of two subs-resonators. In **Figures 4–6** the OPL of the folded MPC is 49.6, 97.6 and 173.6 m under different ray parameters shown in **Table 1**.

In order to validate the calculation model based on the modified ABCD matrix, a comparison of the blue spot patterns in **Figures 7A–9A** simulated by optical software with the red spot patterns **Figures 7B–9B** from the modified ABCD matrix model shows that the consistency between the calculated and simulated spot patterns demonstrates the validity of the modified 4×4 ABCD matrix with the astigmatism of the off-axis mirror. It is found that the slight difference between **Figures 9A,B** mainly results from the ABCD matrix's paraxial approximation error which is amplified in hundreds of cycles. For non-paraxial rays, the paraxial approximation error will make the spot pattern seriously distorted in multiple cycles.

CONCLUSION

In conclusion, a new folded MPC and a modified ABCD matrix with astigmatism are proposed. The spot patterns from the calculation model and optical software show that the new folded MPC is powerful to the long OPL with rich spot patterns, which are very same as the cylindrical and astigmatic MPC. For the new MPC, the excellent ratio of the total OPL to the volume can realize a highly sensitive and compact gas sensor with a low cost due to the use of a common spherical mirror and plane

mirror to form two subs-MPCs. Compact or portable MPCs such as the one displayed on paper have many uses in various fields such as climate change, atmospheric monitoring, and medical diagnostics. Further topics of interest include the manufacture and testing of the folded MPC, as well as the investigation of laser beam spot interference and thermal stability of the folded MPC of this type.

DATA AVAILABILITY STATEMENT

The original contributions presented in the study are included in the article/supplementary material, further inquiries can be directed to the corresponding author.

AUTHOR CONTRIBUTIONS

GC, Y-NC, XT, J-JC, and J-JW contributed to the writing of the manuscript and to the interpretation of results. GC: Conceptualization, Writing-Original draft preparation. Y-NC and XT: Software, Validation. J-JC and J-JW: Writing-Reviewing and Editing.

FUNDING

This research was funded by the Natural Science Foundation of Anhui Province (Grant Nos. 202004a07020046 and 1908085QD156); National Natural Science Foundation of China (NSFC) (Grant No. 62105005); Foundation of State Key Laboratory of Mining Response and Disaster Prevention and Control in Deep Coal Mines (Grant No SKLMRDPC19KF12); Research Foundation of the Institute of Environment-Friendly Materials and Occupational Health of Anhui University of Science and Technology (Wuhu) (Grant No. ALW2020YF04) for support.

REFERENCES

- Ma Y, He Y, Tong Y, Yu X, Tittel FK. Quartz-tuning-fork Enhanced Photothermal Spectroscopy for Ultra-high Sensitive Trace Gas Detection. *Opt. Express* (2018) 26:32103–10. doi:10.1364/OE.26.032103
- Wysocki G, Bakhirkin Y, So S, Tittel FK, Hill CJ, Yang RQ, et al. Dual Interband Cascade Laser Based Trace-Gas Sensor for Environmental Monitoring. *Appl. Opt.* (2007) 46:8202–10. doi:10.1364/ao.46.008202
- Linnerud I, Kaspersen P, Jaeger T. Gas Monitoring in the Process Industry Using Diode Laser Spectroscopy. *Appl Phys B Lasers Opt* (1998) 67:297–305. doi:10.1007/s003400050509
- Lang Z, Qiao S, Ma Y. Acoustic Microresonator Based In-Plane Quartz-Enhanced Photoacoustic Spectroscopy Sensor with a Line Interaction Mode. *Opt. Lett.* (2022) 47:1295–8. doi:10.1364/OL.452085
- Zou J, Wang F. Simultaneous Measurement of SO₂ and NO₂ Concentration Using an Optical Fiber-Based LP-DOAS System. *中国光学快报* (2020) 18:021201–33. doi:10.3788/COL202018.021201
- Ma Y, Lewicki R, Razeghi M, Tittel FK. QEPAS Based Ppb-Level Detection of CO and N₂O Using a High Power CW DFB-QCL. *Opt. Express* (2013) 21:1008–19. doi:10.1364/OE.21.001008
- Tittel FK. Current Status of Midinfrared Quantum and Interband Cascade Lasers for Clinical Breath Analysis. *Opt. Eng* (2010) 49:111123. doi:10.1117/1.3498768
- Werle P, Mucke R, Slemr F. The Limits of Signal Averaging in Atmospheric Trace-Gas Monitoring by Tunable Diode-Laser Absorption Spectroscopy (Tdlas). *Appl. Phys. B* (1993) 57:131–9. doi:10.1007/BF00425997
- Liu X, Ma Y. Sensitive Carbon Monoxide Detection Based on Light-Induced Thermoelastic Spectroscopy with a Fiber-Coupled Multipass Cell [Invited]. *中国光学快报* (2022) 20:031201. doi:10.3788/COL202220.031201
- Weibring P, Richter D, Fried A, Walega JG, Dyroff C. Ultra-high-precision Mid-IR Spectrometer II: System Description and Spectroscopic Performance. *Appl. Phys. B* (2006) 85:207–18. doi:10.1007/s00340-006-2300-4
- White JU. Long Optical Paths of Large Aperture. *J. Opt. Soc. Am.* (1942) 32:285–7. doi:10.1364/josa.32.000285
- Chernin SM, Barskaya EG. Optical Multipass Matrix Systems. *Appl. Opt.* (1991) 30:51–8. doi:10.1364/AO.30.000051
- Herriott D, Kogelnik H, Kompfner R. Off-Axis Paths in Spherical Mirror Interferometers. *Appl. Opt.* (1964) 3:523–6. doi:10.1364/AO.3.000523
- Tuzson B, Mangold M, Looser H, Manninen A, Emmenegger L. Compact Multipass Optical Cell for Laser Spectroscopy. *Opt. Lett.* (2013) 38:257–9. doi:10.1364/OL.38.000257
- Mangold M, Tuzson B, Hundt M, Jágerská J, Looser H, Emmenegger L. Circular Paraboloid Reflection Cell for Laser Spectroscopic Trace Gas Analysis. *J. Opt. Soc. Am. A* (2016) 33:913–9. doi:10.1364/JOSAA.33.000913
- Liu K, Wang L, Tan T, Wang G, Zhang W, Chen W, et al. Highly Sensitive Detection of Methane by Near-Infrared Laser Absorption Spectroscopy Using a Compact Dense-Pattern Multipass Cell. *Sensors Actuators B Chem* (2015) 220:1000–5. doi:10.1016/j.snb.2015.05.136
- Dong L, Li C, Sanchez NP, Gluszek AK, Griffin RJ, Tittel FK. Compact CH₄ Sensor System Based on a Continuous-Wave, Low Power Consumption, Room Temperature Interband Cascade Laser. *Appl. Phys. Lett.* (2016) 108:011106. doi:10.1063/1.4939452
- Dong L, Yu Y, Li C, So S, Tittel FK. Ppb-level Formaldehyde Detection Using a CW Room-Temperature Interband Cascade Laser and a Miniature Dense Pattern Multipass Gas Cell. *Opt. Express* (2015) 23:19821–30. doi:10.1364/OE.23.019821
- Dong L, Tittel FK, Li C, Sanchez NP, Wu H, Zheng C, et al. Compact Tdlas Based Sensor Design Using Interband Cascade Lasers for Mid-IR Trace Gas Sensing. *Opt. Express* (2016) 24:A528–A535. doi:10.1364/OE.24.00A528
- Ozharar S, Sennaroglu A. Mirrors with Designed Spherical Aberration for Multi-Pass Cavities. *Opt. Lett.* (2017) 42:1935–8. doi:10.1364/OL.42.001935
- Kong R, Sun T, Liu P, Zhou X. Optical Design and Analysis of a Two-Spherical-Mirror-Based Multipass Cell. *Appl. Opt.* (2020) 59:1545–52. doi:10.1364/AO.381632
- Cui R, Dong L, Wu H, Li S, Yin X, Zhang L, et al. Calculation Model of Dense Spot Pattern Multi-Pass Cells Based on a Spherical Mirror Aberration. *Opt. Lett.* (2019) 44:1108–11. doi:10.1364/OL.44.001108
- Li S, Sun L. Natural Logarithm Wavelength Modulation Spectroscopy. *Chin Opt Lett* (2021) 19:031201. doi:10.3788/col202119.031201

Conflict of Interest: The authors declare that the research was conducted in the absence of any commercial or financial relationships that could be construed as a potential conflict of interest.

Publisher's Note: All claims expressed in this article are solely those of the authors and do not necessarily represent those of their affiliated organizations, or those of the publisher, the editors and the reviewers. Any product that may be evaluated in this article, or claim that may be made by its manufacturer, is not guaranteed or endorsed by the publisher.

Copyright © 2022 Cheng, Cao, Tian, Chen and Wang. This is an open-access article distributed under the terms of the Creative Commons Attribution License (CC BY). The use, distribution or reproduction in other forums is permitted, provided the original author(s) and the copyright owner(s) are credited and that the original publication in this journal is cited, in accordance with accepted academic practice. No use, distribution or reproduction is permitted which does not comply with these terms.